Development 138, 2783-2792 (2011) doi:10.1242/dev.063834

Evolutionary plasticity of segmentation clock networks

Aurélie J. Krol[1,2,*], Daniela Roellig[3,*], Mary-Lee Dequéant[1,*], Olivier Tassy[1,2,4,*], Earl Glynn[1], Gaye Hattem[1], Arcady Mushegian[1], Andrew C. Oates[3] and Olivier Pourquié[1,2,4,†]

SUMMARY

The vertebral column is a conserved anatomical structure that defines the vertebrate phylum. The periodic or segmental pattern of the vertebral column is established early in development when the vertebral precursors, the somites, are rhythmically produced from presomitic mesoderm (PSM). This rhythmic activity is controlled by a segmentation clock that is associated with the periodic transcription of cyclic genes in the PSM. Comparison of the mouse, chicken and zebrafish PSM oscillatory transcriptomes revealed networks of 40 to 100 cyclic genes mostly involved in Notch, Wnt and FGF signaling pathways. However, despite this conserved signaling oscillation, the identity of individual cyclic genes mostly differed between the three species, indicating a surprising evolutionary plasticity of the segmentation networks.

KEY WORDS: Somitogenesis, Segmentation, Evolution, Cyclic genes, Segmentation clock, Microarray, Chicken, Zebrafish, Mouse, Notch, Wnt, FGF

INTRODUCTION

The periodic organization of the vertebrate body, which is most visible in the vertebrae, is established during embryogenesis. In vertebrates, a complex signaling pulse from the segmentation clock generates a rhythmic wave of gene expression that controls the periodic specification of vertebral precursors (Dequeant and Pourquie, 2008). More than 40 cyclic genes with this oscillatory behavior, mostly encoding members and targets of the Notch, FGF and Wnt signaling pathways, have been identified in mouse using a microarray approach (Dequeant et al., 2006). Many of these genes encode negative-feedback inhibitors of the pathways, and current models suggest that these feedbacks might be important for oscillations (Goldbeter and Pourquie, 2008; Lewis, 2003). Cyclic genes have also been identified by a candidate gene approach in other species such as chicken (Aulehla and Johnson, 1999; Dale et al., 2006; Jouve et al., 2000; Leimeister et al., 2000; McGrew et al., 1998; Palmeirim et al., 1997; Wright et al., 2009), zebrafish (Henry et al., 2002; Holley et al., 2000; Jiang et al., 2000; Oates and Ho, 2002; Shankaran et al., 2007; Sieger et al., 2004) and *Xenopus* (Li et al., 2003), indicating an evolutionary conservation of the segmentation clock in vertebrates. In these species, the few known cyclic genes mostly belong to the Notch pathway, including members of the Hairy and enhancer of split (Hes/Her) family of bHLH transcription factors and the Notch glycosyl transferase lunatic fringe (*Lfng*).

A systematic investigation of cyclic genes in different species is crucial for understanding the molecular evolution of the segmentation clock and might also provide insight into the mechanism of the clock in extant species. Here, we performed a genome-wide search to identify and compare the sets of cyclic genes associated with the segmentation clock in three vertebrate species: mouse (*Mus musculus*), chicken (*Gallus gallus*) and zebrafish (*Danio rerio*). We find that the cyclic gene networks for the three species consist of 40 to 100 genes. We further show that despite an overall conservation of rhythmic pathway activation, the identity of cyclic genes within each pathway differs between species. Surprisingly, conservation of cyclic genes for all three species is limited to orthologs of the Hes/Her transcriptional repressors.

[1]Stowers Institute for Medical Research, Kansas City, MO 64110, USA. [2]Institut de Génétique et de Biologie Moléculaire et Cellulaire (IGBMC), CNRS (UMR 7104), Inserm U964, Université de Strasbourg, Illkirch F-67400, France. [3]Max Planck Institute of Molecular Cell Biology and Genetics, 01307 Dresden, Germany. [4]Howard Hughes Medical Institute, Kansas City, MO 64110, USA.

*These authors contributed equally to this work
†Author for correspondence (pourquie@igbmc.fr)

Accepted 26 April 2011

MATERIALS AND METHODS

Dissection of embryonic PSM tissue

Mouse embryos were dissected as described (Dequeant et al., 2006). Fertilized chicken eggs were obtained from Ozark Hatcheries (Neosho, MO, USA) and incubated at 38°C in a humidified incubator. Two-day-old chicken embryos [15- or 16-somite stage, 12HH (Hamburger and Hamilton, 1992)] were dissected in cold Tyrode solution made with DEPC-treated water under RNase-free conditions. After being cut out of the egg, the embryos were pinned in a silicone-covered Petri dish, ventral side up, and treated with pancreatin (4xUSP, Invitrogen). The endoderm was removed, and the right posterior half of the PSM (measured with a reticule) was separated from the surrounding structures with a tungsten needle. Zebrafish embryos were obtained from natural AB strain crosses [Zebrafish International Resource Center (ZIRC), University of Oregon] and maintained at 28.5°C. Dissection at the 12- and 13-somite stage was performed as described (Picker et al., 2009). The PSM pieces excised from chicken and zebrafish were stored in Trizol (Invitrogen) at –80°C for subsequent RNA extraction. The remaining embryo portion, including the contralateral PSM side, was fixed immediately.

In situ hybridization (ISH)

ISH was performed as described (Henrique et al., 1995; Thisse et al., 1993). Whole-mount ISH for candidate cyclic gene validation was performed on at least ten embryos for each probe to look for a dynamic pattern of expression in the PSM. Probe references and primers for PCR-based probe preparation are listed in Table S1 in the supplementary material. PCR was performed using standard conditions.

RNA preparation and microarray hybridization

RNA was extracted from the dissected PSM piece and amplified before hybridization of each sample individually on an Affymetrix GeneChip array. The RNA samples extracted from mouse embryo PSM as described (Dequeant et al., 2006) were amplified using the first cycle of

the GeneChip Eukaryotic Small Sample Target Labeling Assay version II, and the second cycle of the Two-Cycle Eukaryotic Target Labeling Assay, as described in the Affymetrix GeneChip Expression Analysis Technical Manual rev5. Amplified RNA samples were hybridized to Affymetrix GeneChip Mouse Genome 430 2.0 arrays. For chicken and zebrafish, total RNA was extracted from PSM pieces using Trizol. PSM pieces contained ~4000 chicken cells or ~400 zebrafish cells. The mRNA of each sample was amplified following a two-cycle linear amplification protocol as described in the Two-Cycle Eukaryotic Target Labeling Assay in the Affymetrix GeneChip Expression Analysis Technical Manual rev5. Briefly, cDNA was synthesized from total RNA using T7 linked to oligo(dT) primers. After second-strand synthesis, cRNA was in vitro transcribed using unlabeled ribonucleotides. Upon a second round of cDNA synthesis using random priming, cRNA was made with biotin-labeled CTP and UTP, yielding 35-135 μg of biotinylated cRNA for chicken and 3-6 μg for zebrafish. RNA quality was checked after the second round of amplification by measuring the A_{260}/A_{280} ratio (which ranged from 1.8 to 2.1) and the fragment size with the Agilent Bioanalyser (mean size >1 kb).

Five micrograms of RNA from good quality samples was fragmented to less than 200 bp, hybridized to Affymetrix GeneChip chicken genome arrays or GeneChip zebrafish genome arrays according to manufacturer's instructions and scanned with a GeneArray scanner (Agilent G2500A) at the Microarray Core Facility of the Stowers Institute for Medical Research. The array readout was processed using Affymetrix Microarray Suite (MAS) 5.0 and scaled by adjusting the average intensity of each array to a target intensity of 150. The quality control parameters from the Affymetrix array reports were within acceptable limits and highly similar between the arrays. The raw data are available on ArrayExpress with accession E-MTAB-406. Non-biological variance of the microarrays was controlled by two methods: the R package affyPLM (Bolstad et al., 2005) using the normalized unscaled standard error (NUSE) and relative expression (RLE) functions; and principal component analysis (PCA) using Partek Genomics Suite. Arrays exhibiting reduced quality levels and those deviating significantly from the others were removed.

Filtration of the datasets

Identical primary filtration steps were applied to all microarray series. Probesets called 'absent' by detection call (provided by MAS5) for more than half of the samples of a microarray series were removed. For the three species, probesets with a maximum intensity below 29 were removed [based on a validated cyclic zebrafish gene (*her4*) with the smallest value of maximum intensity among all three species].

Secondary filtration steps differed among species. For mouse secondary filtration, we used the overlap of the candidate cyclic genes from mouse1 and mouse2. For chicken and zebrafish, only one dataset was available and each dataset was filtered using expression thresholds of known or validated cyclic genes from the respective species (see Table S2 in the supplementary material). Probesets called 'present' in at least 18 samples for chicken and 14 samples for zebrafish were retained. Probesets with maximum intensity values of ≥655.8 for chicken and ≥29 for zebrafish and those with a peak-to-trough (PT) amplitude (maximum expression value over minimum expression value) ≥1.30 for chicken and ≥4.54 for zebrafish were retained.

Candidate cyclic gene expression analysis by quantitative (q) PCR

Similar to the microarray time series, the right-hand side of the posterior PSM was dissected from a series of embryos and processed for qPCR analysis. The remainder of the embryo was hybridized in whole-mount with a *Lfng* riboprobe for mouse and chicken and *her7* for zebrafish. Ten mouse or chicken embryos and 16 zebrafish embryos representing a complete oscillation cycle were selected. Total RNA was extracted from the samples as described above. cDNA was synthesized using the High Capacity RNA to cDNA Kit from ABI in 40 μl reactions.

qPCR of mouse and chicken targets was performed with 0.2 μl cDNA mixed with 2× Power SYBR Green (Applied Biosystems) with 0.4 μM primers in a total volume of 20 μl. qPCR reactions were run on the ABI 7900HT Real-Time PCR System using 7900 System SDS software. Each sample was run in technical triplicate and *Gapdh* and β-actin (*Actb*) were used as control genes. Thermal cycling conditions were as follows: enzyme activation for 10 minutes at 95°C, then 40 cycles of denaturation at 95°C and annealing/extension for 60 seconds at 60°C.

For zebrafish targets, 2.5 μl zebrafish cDNA was mixed with 2× Fast SYBR Green Master Mix solution (Applied Biosystems) with 0.4 μM primers in a total reaction volume of 20 μl. qPCR reactions were run on a 7500 Fast Real-Time PCR System (ABI 7500HT, Applied Biosystems) using the 7500 Fast System SDS software. Thermal cycling conditions were as follows: enzyme activation for 20 seconds at 95°C, then 40 cycles of denaturation for 3 seconds at 95°C and annealing/extension for 30 seconds at 60°C. After a pilot test on cDNA from zebrafish PSM using β*actin1*, β*actin2*, *ef1a*, *rpl13* and *hprt1* (McCurley and Callard, 2008; Tang et al., 2007b), β*actin1* was selected as the reference gene as it showed the least variation between samples and had Ct values comparable to those of genes of interest. All zebrafish samples were run in technical duplicate, and several genes (*her1*, *her7*, *tbx16*) were confirmed with biological duplicates.

Primers for all three species are listed in Table S3 in the supplementary material. The mean Ct of each group of two or three replicates was used to calculate the ΔCt values ($Ct_{\text{gene of interest}} - Ct_{\text{reference gene}}$). We calculated the $\log_2$ ratios of each ΔCt value normalized to the mean ΔCt value over all time points. A profile was considered cyclic if the PT amplitude was at least 0.4 fold, the Lomb-Scargle *P*-value less than 0.5 (the small sample number gives elevated *P*-values) and the profile had at least four consecutive points with either positive or negative $\log_2$ ratios with phase corresponding to the ISH embryo phase ordering. The qPCR protocol was first validated using the known cyclic genes *Lfng* in both mouse and chicken, *Dkk1* in mouse, and *her1* and *her7* in zebrafish.

Manteia

Owing to the poor quality of probeset annotations for chicken and zebrafish, we developed a new database called Manteia. This system allows each microarray probeset to be mapped to the corresponding gene models from Ensembl (Hubbard et al., 2009) and Entrez (Maglott et al., 2007) in order to use their annotations to name and annotate the relevant probesets in our study. The mapping is based on annotation files provided by Ensembl, NCBI and Affymetrix. Additional functional annotations are obtained from MGI (Bult et al., 2008), ZFIN (Sprague et al., 2006), DBD (Wilson et al., 2008) and KEGG (Kanehisa et al., 2010) by mapping their respective data to the corresponding Ensembl and Entrez gene models in Manteia.

The conservation analysis among mouse, chicken and zebrafish was based on ortholog predictions performed with InParanoid (Berglund et al., 2008) and Ensembl Compara. This prediction was used in Manteia to identify and re-annotate poorly annotated gene models using their ortholog data. The Gene Ontology (GO) distribution analysis used a dedicated data-mining system based on GO annotations from Ensembl, Entrez and KEGG in combination with the GO ontology graph from the GO consortium (Ashburner et al., 2000). The GO enrichment analysis was performed in Manteia using its statistical module, which works similarly to GoMiner (Zeeberg et al., 2003): gene annotations from a dataset were extracted from the database taking into account the dependencies between the GO terms. The occurrence of each term in this dataset was then compared with the occurrence of the same terms from the annotation of all the genes present on the microarray. A *P*-value was computed using a hypergeometric test to evaluate the significance of the differences observed in these distributions. These *P*-values were corrected for multiple testing using the Benjamini-Hochberg false data rate correction (Benjamini et al., 2001). Terms were considered significant when the false data rate was below 5% and when they were linked to more than 5% of the genes. No significant difference in the distribution was observed when only the original GO annotations were used (see Fig. S3A in the supplementary material) as compared with when the GO terms were inferred from their human and mouse orthologs (see Fig. S3B in the supplementary material).

The Manteia database was developed under PostgreSQL 8. The web site and the annotation pipeline were written in PHP 5. Manteia is available at http://manteia.igbmc.fr and is free to use for academic purposes. For more information, see Ozbudak et al. (Ozbudak et al., 2010).

RESULTS

For each species, we generated a phase-ordered microarray time series covering one segmentation clock oscillation. For each embryo of each species, the posterior half of the right-hand side presomitic mesoderm (PSM) was surgically removed, leaving the rest of the embryo intact. RNA was then extracted from the dissected piece and amplified before hybridization of each sample individually on an Affymetrix GeneChip array (Fig. 1A). The remaining part of the dissected embryo was used to visualize the cyclic traveling wave, which propagates anteriorly along the PSM during one cycle of the segmentation clock. These dynamic stripes were detected by in situ hybridization (ISH) with the known cyclic genes *Lfng* for mouse and chick (Aulehla and Johnson, 1999; McGrew et al., 1998) and *her7* (Oates and Ho, 2002) for zebrafish. Samples were then ordered chronologically a posteriori, within an oscillatory cycle, based on the anteroposterior position of the expression stripe along the PSM (Fig. 1B-D). Twenty-two out of 80 dissected 15- to 16-somite stage chicken embryos and 25 out of 100 dissected 12- to 13-somite stage zebrafish embryos were selected on the basis of successful surgery and ISH to represent one complete oscillation cycle. For both chicken and zebrafish embryos, the mRNA of each sample was amplified following a two-cycle linear amplification protocol and hybridized on Affymetrix chips. For mouse embryos, the original samples described by Dequeant et al. (Dequeant et al., 2006) (here termed mouse1), which had been hybridized to the GeneChip Mouse 430A array, were reamplified and hybridized to the new whole-genome GeneChip Mouse 430.2 array (called mouse2), providing a comprehensive survey of the mouse genome and a form of technical replicate of the original time series. Following quality controls of the microarray data, we selected 20 out of 20 hybridized arrays for mouse1, 16 out of 20 hybridized arrays for mouse2, 18 out of 22 hybridized arrays for chicken, and 21 out of 25 hybridized arrays for zebrafish for subsequent analysis. We first analyzed the expression of known cyclic genes (*Hes1* and *Hes5* for mouse and chicken and *her7* and *her15* for zebrafish) in the three time series (Fig. 1B-D). We observed a clear cyclic behavior correlating with the ISH phases for all three species, supporting the good quality of the datasets.

For the primary analysis of the datasets, cyclic profiles were identified using an algorithm based on Fourier analysis that assigns a significance value for the periodicity of each probeset expression profile (Dequeant et al., 2006; Glynn et al., 2006). Additionally, a permutation-based algorithm (Fig. 2A) was applied to distinguish stable periodic expression profiles of candidate cyclic genes from periodic profiles arising from random noise. We created 10^4 permutations of the datasets, in which each embryo position within the oscillatory cycle was allowed to vary within a local time window (see Fig. S1 in the supplementary material). For each experimental dataset, a randomized control dataset with the same distribution, mean and variance was generated by resampling microarray expression values with replacement, i.e. the intensity values within each microarray were randomly exchanged. We also generated a synthetic control dataset with ~2.5% perfect sinusoidal expression patterns in order to see how perfectly periodic genes stand out from a random dataset (Fig. 3B). The randomized datasets were subjected to the same 10^4 random permutations as the experimental datasets. After each round of permutation, a Lomb-Scargle algorithm (Dequeant et al., 2006; Glynn et al., 2006) was applied to obtain a significance value (*P*-value) for the periodicity of each probeset profile. For each probeset, a rank product was calculated from the ranks of its *P*-values after each round of permutation (Fig. 3). To exclude non-expressed or non-reliably detected genes from the analysis, we applied a primary filtration at this step: for microarray sets of all three species only those probesets detected as present by detection call in at least half of the samples and with a maximum intensity higher than 29 were retained for further analysis. We then performed *t*-tests on the distribution of *P*-values between each similarly ranked probeset from the dataset and the corresponding randomized dataset. The upper limit to the number of cyclic candidates was determined by the first rank where the *P*-value of the *t*-test was higher than 0.01 (Fig. 4). This identified 353 candidate

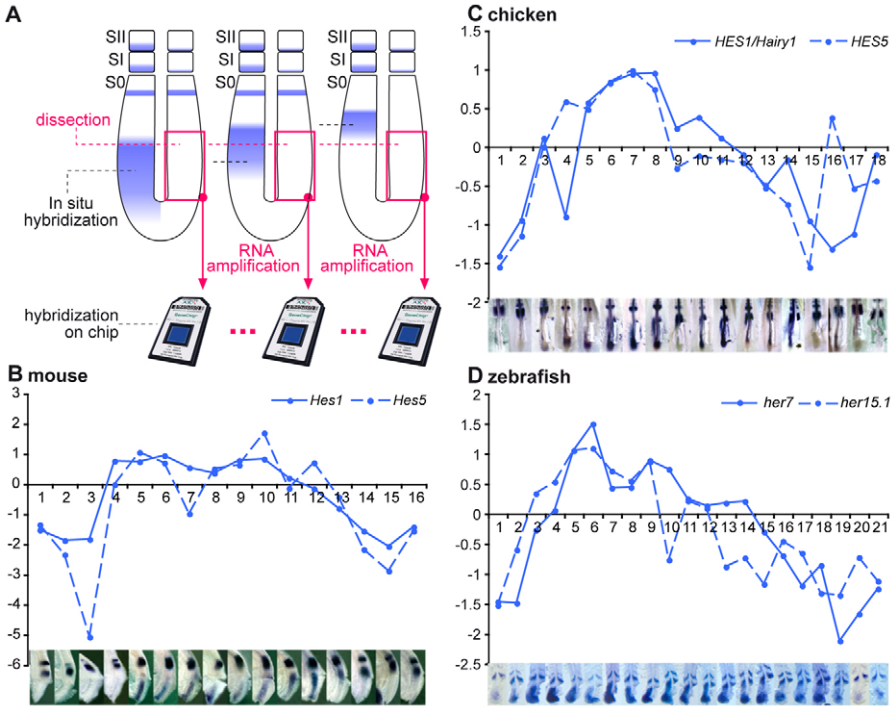

Fig. 1. Identification of cyclic genes from mouse, chicken and zebrafish using microarray time series. (**A**) Experimental procedure. The right posterior half of the presomitic mesoderm (PSM) was surgically removed from zebrafish, chicken or mouse embryos. Total RNA was extracted, amplified and hybridized to Affymetrix microarrays. Dissected embryos were ordered along one segmentation clock cycle using the position of cyclic gene expression domains [*Lfng* mouse and chicken, *her7* zebrafish, detected by in situ hybridization (ISH)] along the anteroposterior axis of the left PSM. The microarrays corresponding to the dissected samples were ordered accordingly. (**B-D**) Microarray expression profiles of the known cyclic genes *Hes1* and *Hes5* for mouse (B) and chicken (C) and *her7* and *her15* for zebrafish (D) and corresponding ISH of the dissected embryos (bottom). The *x*-axis corresponds to the sample number and the *y*-axis to the $\log_2$ ratios of the expression profiles.

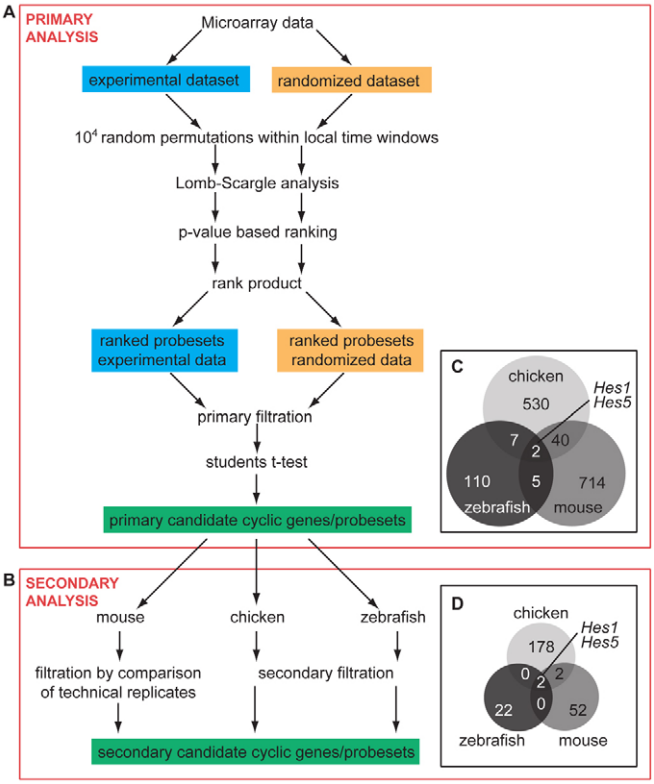

Fig. 2. Workflow for the identification of candidate cyclic genes. (**A**) A primary analysis was first carried out to identify candidate cyclic genes based on the periodicity of their expression profile in the microarray series. A permutation algorithm that compares the experimental datasets with randomized datasets was used to identify the cyclic genes in the three species. Local time windows (groups shown in Fig. S2 in the supplementary material), within which the exact ordering of the samples based on the phase of the oscillation is hard to ascertain, were first defined. Then, 10^4 permutations within these defined windows were created for each dataset. We next applied the Lomb-Scargle (L-S) algorithm, which is a Fourier-related analysis, to each permutation to rank the candidate cyclic genes based on their periodicity. A global ranking from the most to the least cyclic probeset was computed using the product of the ranks of the 10^4 orderings. A primary filtration was used to remove the non-expressed and non-reliably detected probesets. Finally, the distributions of *P*-values from the experimental and random datasets were compared using a *t*-test. The number of candidate cyclic genes was determined by the first rank where the *t*-test *P*-value was higher than 0.01. (**B**) The secondary analysis for the mouse dataset selects the candidate cyclic genes that are in common between the two mouse microarrays. For chicken and zebrafish, we used as filtration criteria the signal thresholds of known cyclic genes. (**C**,**D**) Venn diagrams illustrate the number and overlap of candidate cyclic genes after primary (C) and secondary (D) analysis.

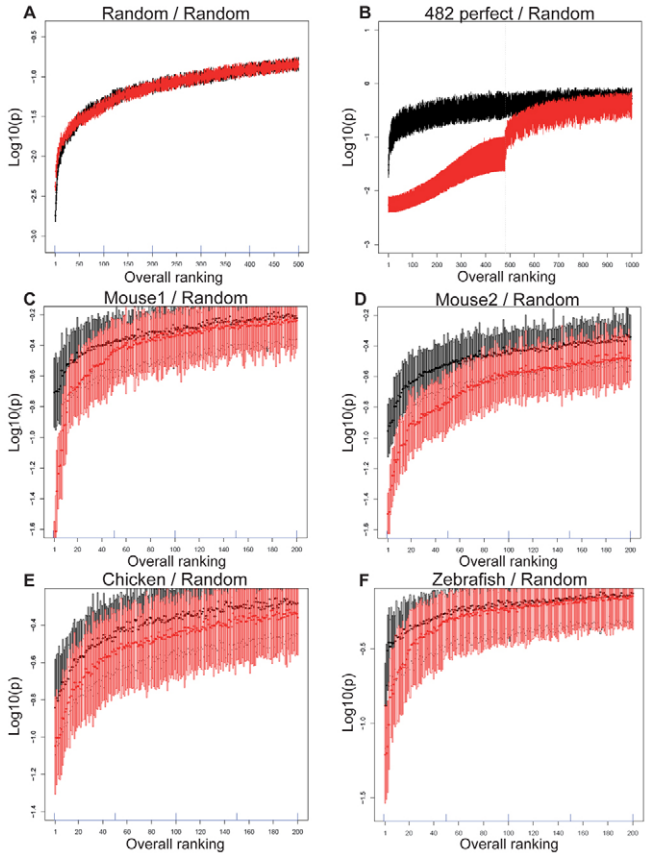

Fig. 3. Comparison of experimental and randomly generated control datasets. *P*-values of the Lomb-Scargle analyses for the 10^4 orderings of the experimental datasets (red) and the randomized dataset (black). Each vertical bar corresponds to the 10^4 *P*-values from one probeset, with the median value as a horizontal line. (**A**) Comparison of a random dataset with another random dataset shows almost perfect overlap. (**B**) Comparison of a randomized dataset (black) with a synthetic positive control dataset of 20,000 genes containing 482 (~2.5%) perfectly periodic genes (sinusoidal curves with slight phase shifts, but similar amplitude). The remaining 19,528 expression profiles are Gaussian noise (red). (**C-F**) Comparison of experimental datasets and the corresponding randomized datasets for mouse1 (C), mouse2 (D), chicken (E) and zebrafish (F) microarrays series. Note that the scale on the axes varies between panels.

cyclic probesets corresponding to 322 annotated genes in the mouse1 dataset, 999 probesets (764 genes) in the mouse2 dataset, 869 probesets (580 genes) in chicken, and 152 probesets (124 genes) in zebrafish (see Table S4 in the supplementary material).

Distinct clusters of mouse cyclic genes with opposing phase

To estimate the contribution of noise to these candidate cyclic gene lists we applied a secondary filtration step, taking advantage of the technical replicate of the mouse dataset (Fig. 2B). Comparison of the 322 cyclic candidates of the mouse1 dataset (Dequeant et al., 2006) with the 764 mouse2 cyclic candidates revealed that only 64 cyclic candidates are common to both datasets. Most validated cyclic genes associated with Notch, FGF or Wnt signaling (Dequeant et al., 2006) were among the 64 genes common to the mouse1 and mouse2 datasets. As expected, these genes define two clusters with opposite expression phases, one enriched in Notch- and FGF-associated genes and the other in genes related to the Wnt signaling pathway (Fig. 5A). We reasoned that common candidates were more likely to reflect true positives if they were found in the same cluster in mouse1 and mouse2. Using the conservation of the expression phase, we identified 56 genes as highly robust candidates for genuine cyclic genes (Fig. 5A and see Table S5 in the supplementary material). This corresponds to ~17% of the 322 genes of the mouse1 list. From the 764 candidate cyclic genes identified in the mouse2 analysis, 152 are specific to the new Mouse 430.2 microarray; therefore, we predict

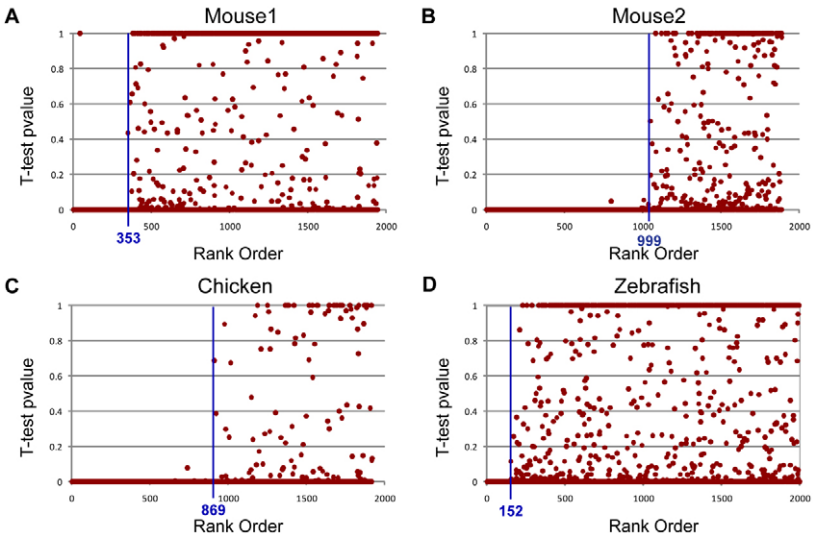

Fig. 4. Estimation of the number of candidate cyclic probesets in each species. *P*-values of the *t*-test comparing the experimental datasets with the random datasets, as a function of the rank order for (**A**) mouse1, (**B**) mouse2, (**C**) chicken and (**D**) zebrafish. The cut-off was placed at the first rank where the *P*-value was higher than 0.01 (a few outliers with *P*-values higher than 0.01 before the cut-off were not taken into consideration).

the existence of another 26 cyclic genes (17% of 152 genes), yielding a total of 82 cyclic gene candidates in the mouse. These cyclic genes include *Hes1*, *Hes5*, *Hey1*, *Id1* and *Efna1* for Notch and *Spry2*, *Bcl2l11* and *Egr1* for FGF/MAPK. The zinc-finger transcription factor *Klf10*, not previously associated with Notch or FGF signaling, was found in the Notch/FGF cluster in the two analyses, as was the FGF target *Ier2* (Hong and Dawid, 2009). Wnt-associated genes identified in both analyses include *Axin2*, *Dkk1*, *Dact1*, *Sp5*, *Myc*, *Tnfrsf19*, *Cyr61* and *Shisa2* (Dequeant et al., 2006; Furushima et al., 2007; Latinkic et al., 2003). Additional candidate cyclic genes with Notch, FGF or Wnt association were found in mouse2 (Table 1). This analysis significantly extends the list of mouse cyclic genes and suggests that the general logic of the mouse gene network is restricted to the Notch/FGF cluster and the Wnt cluster oscillating in anti-phase.

Conserved rhythmic expression of Notch, FGF and Wnt signaling pathway genes in amniotes

Assuming a similar proportion of false positives as in the mouse datasets predicts ~100 cyclic genes in chicken. To enrich the list of 580 candidates for true positives, we filtered the data using signal thresholds from known or validated chicken cyclic genes (secondary filtration; Fig. 2B and see Table S2 in the supplementary material) and recovered 182 genes (see Table S5 in the supplementary material). These segregated into two clusters in opposite expression phases, as observed for the mouse dataset (Fig. 5B). No cyclic gene of the Wnt pathway had previously been reported in chicken; however, our analysis revealed one cluster with several Wnt-associated genes, whereas the other was enriched in Notch-associated genes. The Wnt targets *AXIN2* and *T*, as well as *GPR177* (Wntless), which is involved in Wnt secretion, and the Wnt pathway negative regulator *RRM2* (Tang et al., 2007a) were identified as candidate cyclic genes. FGF-associated genes such as *RAF1*, *MAP2K2* (*ERK*) and *DUSP6* were found in both clusters. Combined, these data show that rhythmic activation of Notch, FGF and Wnt signaling in the PSM is conserved in amniotes.

Limited conservation of individual cyclic genes in amniotes

Strikingly, the Notch, FGF and Wnt signaling-related genes identified as cyclic in chicken differed substantially from those in mouse (Fig. 6A-D). We compared the mouse orthologs of the 182

Table 1. Mouse2-specific candidate cyclic genes related to Notch, FGF and Wnt

Probeset ID	Gene symbol	Gene name	Reference
Notch			
1444279_at	*Huwe1*	HECT, UBA and WWE domain containing 1	(Zhao, X. et al., 2008)
1452214_at	*Skil*	SKI-like	(Colland et al., 2004)
1435176_a_at	*Id2*	Inhibitor of DNA binding 2	(Liu et al., 2004)
1448008_at	*Ankhd1*	Ankyrin repeat and KH domain containing 1	(Traina et al., 2006)
FGF			
1422021_at	*Spry4*	Sprouty homolog 4 (Drosophila)	(Furthauer et al., 2001)
1448830_at	*Dusp1*	Dual specificity phosphatase 1	(Beltman et al., 1996)
1428834_at	*Dusp4*	Dual specificity phosphatase 4	(Chu et al., 1996)
Wnt			
1448698_at	*Ccnd1*	Cyclin D1	(Issack and Ziff, 1998)
1449845_a_at	*Ephb4*	Eph receptor B4	(Kumar et al., 2009)
1434832_at	*Foxo3a*	Forkhead box O3a	(Dehner et al., 2008)
1440519_at	*Sp8*	Trans-acting transcription factor 8	(Bell et al., 2003)
1430554_at	*Lrig3*	Leucine-rich repeats and immunoglobulin-like domains 3	(Zhao, H. et al., 2008)
1430384_at	*Tle4*	Transducin-like enhancer of split 4, homolog of Drosophila E(spl)	(Burks et al., 2009)

Shown are new Notch, FGF and Wnt candidate cyclic genes identified in the mouse2 dataset, which were not present on the microarray used for the mouse1 dataset.

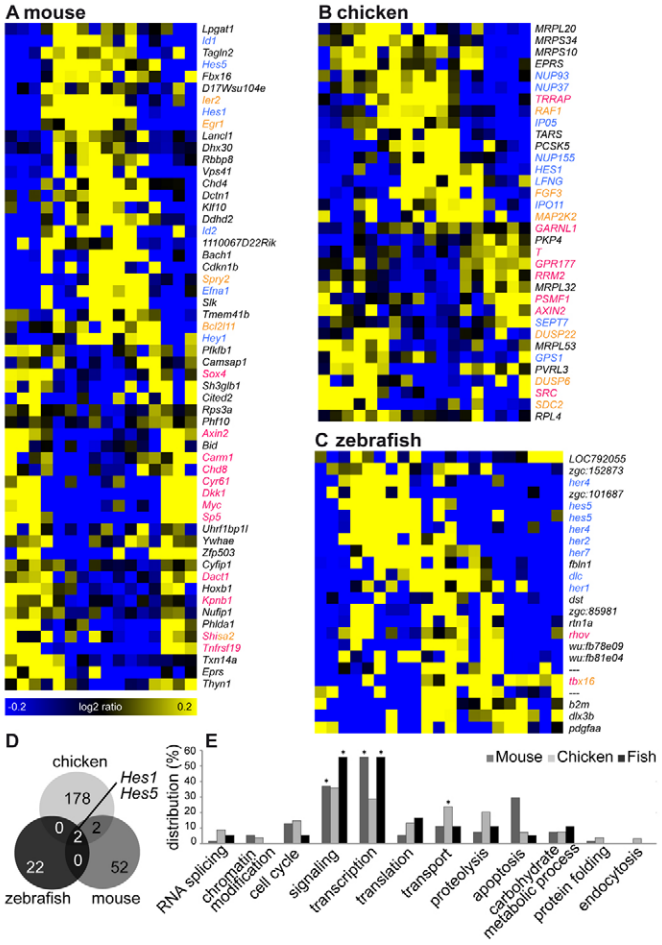

Fig. 5. Cyclic gene candidates mostly belong to the Notch, Wnt and FGF pathways. (**A-C**) Phaseograms of mouse, chicken and zebrafish candidate cyclic genes ordered by time of maximum expression. (A) The 56 candidates shared between mouse1 and mouse2 and sharing a similar phase in the two datasets are shown. (B) Selection of chicken cyclic genes from the candidate list of 182 genes obtained after filtration. (C) Filtered list of 24 cyclic gene candidates from zebrafish. Blue, orange and magenta text indicate association with the Notch, FGF and Wnt pathways, respectively, based on published literature (association with more than one pathway is indicated by mixed color text); other genes are shown in black. (**D**) Venn diagram indicating the number of cyclic genes shared by the three species. (**E**) Percentage of genes annotated with orthology-inferred GO categories in each species. Asterisks indicate when terms related to a category are enriched (P<0.05) in the set.

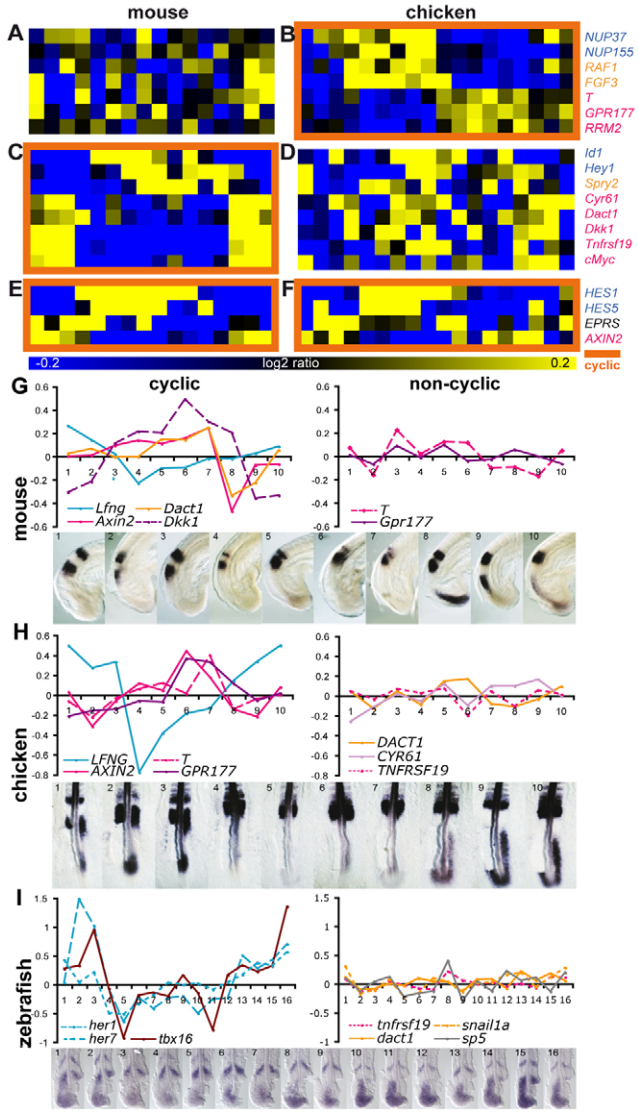

Fig. 6. Lack of conservation of individual cyclic genes between mouse and chicken embryos. (**A-F**) Comparison of genes identified as non-cyclic in mouse (A) but cyclic in chicken (B) and of genes cyclic in mouse (C) but not in chicken (D). Also shown are genes cyclic both in mouse (E) and chicken (F). Orange squares highlight cyclic gene expression time series. Pathway association of candidate cyclic genes is indicated in blue (Notch), orange (FGF) and magenta (Wnt). (**G-I**) qPCR expression profiles (y-axis, $\log_2$ ratio of ΔCt; x-axis, sample number) of cyclic and non-cyclic genes for mouse (G), chicken (H) and zebrafish (I), and ISH of known cyclic genes on dissected embryos used for the qPCR.

expression threshold-filtered chicken genes with the 56 cyclic mouse genes. The overlap was limited, consisting of the Wnt and Notch targets *Axin2*, *Hes1*, *Hes5* and the glutamyl-prolyl-tRNA synthetase *Eprs* (Fig. 6E,F, Fig. 5D). Whereas cyclic *Lfng* expression is known to be conserved between mouse and chicken and was identified in the chicken dataset, it was not recovered from the mouse datasets, most likely owing to insufficient probeset quality. Comparing the 56 mouse cyclic genes with the full chicken list of 580 candidates recovered only two additional matches (*Egr1* and *Txn14a*), further indicating the very limited conservation of cyclic genes between the two species.

We then used quantitative PCR (qPCR) to monitor the periodicity of candidate cyclic genes during one cycle. *Axin2* was detected as periodic by qPCR for both species (Fig. 6G,H). *T* and *Gpr177* were confirmed periodic in chicken, but not in mouse, whereas *Dact1* was periodic in mouse and not in chicken, consistent with the microarray results. Thus, by qPCR, with the exception of *Axin2*, different Wnt-associated genes were found to oscillate in mouse and chicken. Strikingly, we detected no periodic expression of the chicken homologs of *Axin2*, *T*, *Id1*, *Spry2*, *Dact1* and *cMyc* by ISH (see Fig. S2 in the supplementary material) (Gibb et al., 2009), suggesting that ISH is insensitive to small changes in

expression. In summary, we find that although genes from the Notch, FGF and Wnt pathways show cyclic expression in mouse and chicken, different genes from these pathways are detected as periodic in each species.

Divergence of individual cyclic gene expression in zebrafish

Our primary analysis of the zebrafish microarray dataset (Fig. 2A) identified all known cyclic genes represented on the chip: *her1*, *her7*, *her15* and *deltaC*. Anticipating a proportion of false positives similar to mouse, and considering that ~50% of the transcriptome is not on the microarray, we predict ~40 zebrafish cyclic genes. To enrich our candidate cyclic gene list for true positives, we filtered with the signal thresholds of known zebrafish cyclic genes (secondary analysis; Fig. 2B and see Table S2 in the supplementary material) and recovered 24 genes (Fig. 5C and see Table S5 in the supplementary material). We identified the new Notch-associated cyclic genes *her2* and *her4* oscillating in phase with the known cyclic genes *her7* and *her15*. Both *her2* and *her4* showed periodic expression by ISH (see Fig. S2C in the supplementary material). Two entries on this filtered list are associated with FGF and/or Wnt signaling: the T-box transcription factor *tbx16*, which is responsive to both FGF and Wnt (Griffin et al., 1998; Thorpe et al., 2005), and the small GTPase *rhov*, a Wnt target (Guemar et al., 2007). Using qPCR on two independent biological replicates, *tbx16* exhibited an unambiguous periodic profile comparable to that of the positive controls *her1* and *her7* (Fig. 6I). When examined by qPCR and by ISH, the expression of the zebrafish orthologs of the mouse or chicken cyclic genes *nrarpa*, *tnfrsf19*, *sp5*, *sp5-like* and *dact1* did not show a periodic profile (Fig. 6I and see Fig. S2C and Table S6 in the supplementary material). No periodic expression was detected by qPCR for *spry4*, *snail1a*, *dusp6* and *mycb*, nor by ISH for *gpr177*, *spry2*, *dact2*, *myca* and *has2*. Thus, the set of zebrafish cyclic genes appears different from that of mouse and chicken, with a lower total number of cyclic genes and only two associated with FGF and Wnt signaling.

Only *Hes1* and *Hes5* orthologs show cyclic expression in mouse, chicken and zebrafish

Finally, we compared all candidate cyclic genes identified in our analysis from the three datasets (see Table S4 in the supplementary material). To improve the chicken and zebrafish microarray annotation we developed a database, Manteia, which links the Affymetrix probesets to the corresponding NCBI and Ensembl gene models and merges the available information for both (Ozbudak et al., 2010). Mouse orthologs of chicken and zebrafish genes were extracted and compared with mouse2 genes using Manteia. Out of the 56 highly robust mouse candidate genes, 41 orthologs were present on both the mouse2 and chicken microarray, and 41 orthologs were present on both the mouse2 and zebrafish microarray. In total, 34 out of the 56 mouse2 genes have orthologs present on the microarrays of all three species (see Table S7 in the supplementary material). The only cyclic genes common between all three species were the orthologs of the Notch targets *Hes1* and *Hes5* (Fig. 2C,D, Fig. 5D). To investigate the functions of the cyclic genes in the three species, we used their Gene Ontology (GO) annotations and examined a general set of molecular and cellular functions in the filtered gene lists (Fig. 5E and see Fig. S3 in the supplementary material). The GO annotation distribution in these categories was similar between zebrafish, chicken and mouse, with the majority of genes annotated with terms related to signaling pathways and transcription.

DISCUSSION

Our study reports an evolutionary comparison of the cyclic regulation of the transcriptome associated with segmentation in three vertebrate species: zebrafish, chicken and mouse. We were able to identify cyclic networks of 40-100 genes associated with the segmentation clock in these three species. The identified cyclic genes are mostly involved in signaling and transcription. This low number of cyclic genes contrasts with the 3500 genes regulated by the *Arabidopsis* root oscillator (Moreno-Risueno et al., 2010).

The differences between the lists of candidate cyclic genes from the two technical replicates mouse1 and mouse2 indicate a significant false positive rate in these experiments. Several factors might contribute to this experimental noise. First, most cyclic genes show modest oscillatory amplitude. Second, owing to the small size of the microsurgically excised PSM tissue (~500 to 5000 cells), the amount of mRNA isolated is necessarily limited. The two-step amplification required to obtain enough material for hybridization to the arrays might introduce some bias in individual gene expression levels. Third, local errors in assigning the correct phase order to these samples on the basis of in situ expression patterns was likely to have introduced some noise in phase profiles. Because of the difficulty in generating biological or technical replicates for the chicken and zebrafish datasets, we used the level of true positives calculated in mouse to estimate the approximate number of cyclic genes in these two species. In the case of the zebrafish, we made an additional correction because only approximately half the transcriptome is present on the array. Also, it is possible that additional experimental noise deriving from the smaller size of zebrafish PSM samples (~500 cells) contributes to the lower number of cyclic genes estimated in this species relative to amniotes. Despite these experimental constraints, the clear detection of the great majority of previously known cyclic genes in the time series from all three species (Fig. 1B-D), and the confirmation of cyclic expression of additional members of the Notch, FGF and Wnt pathways detected in this analysis by qPCR (Fig. 6G-I), indicate that the statistical analysis we employed allowed the identification of many true positives. Indeed, in the case of zebrafish, all known cyclic genes present on the array were detected as periodically expressed in the dataset.

A striking outcome of this analysis is the identification of zebrafish *tbx16*, which is associated with Wnt and FGF signaling, as a new cyclic gene, raising the possibility that pathways other than Notch oscillate in zebrafish. The zebrafish cyclic gene network might therefore be more similar to that of amniotes than previously thought (Dequeant and Pourquie, 2008), and oscillations of Notch, FGF and Wnt might therefore constitute a conserved feature of vertebrate segmentation (Fig. 7). Nevertheless, we uncovered striking differences between the cyclic gene networks of the three species. Whereas in mouse, cyclic genes segregate into a Notch and FGF pathway-enriched cluster oscillating in opposite phase to a Wnt signaling-enriched cluster, such clear segregation is less evident for chicken and zebrafish. Furthermore, most of the individual cyclic genes associated with the Notch, FGF and Wnt pathways differed among the species. The overlap between the amniotes and zebrafish cyclic gene set is strikingly limited to *Hes1* and *Hes5* orthologs. The segmentation clock has been proposed to rely on a Hes/Her-based negative-feedback loop driving oscillations by delayed transcriptional repression (Bessho et al., 2003; Lewis, 2003). In the case of the Hes/Her genes, the observed conservation of transcript oscillations might be due to their specific

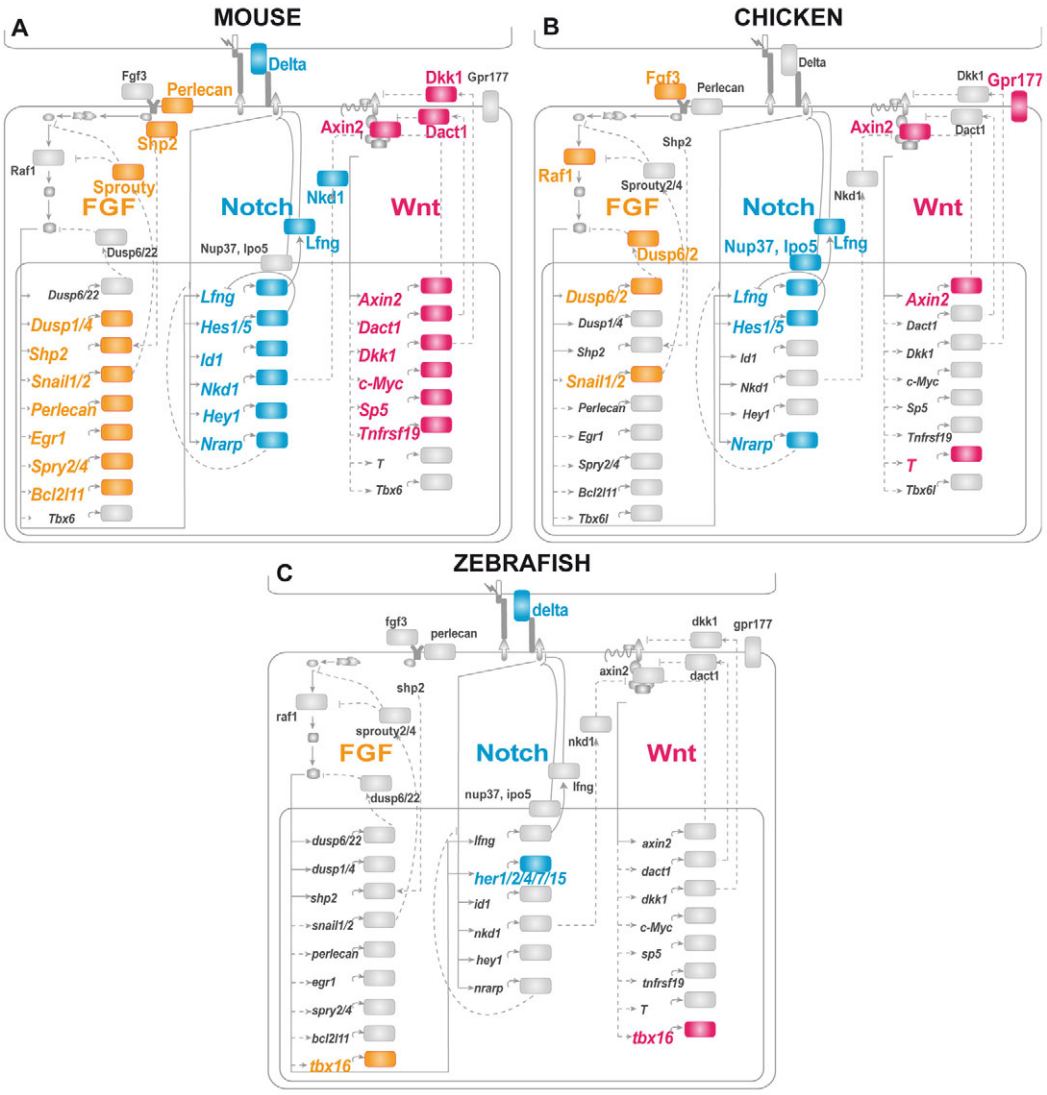

Fig. 7. Comparative pathway networks of cyclic genes in mouse, chicken and zebrafish. Schematic description of one PSM cell interacting with its neighbor, showing the candidate cyclic genes in the Notch, FGF and Wnt signaling pathways identified from (**A**) mouse, (**B**) chicken and (**C**) zebrafish. Cyclic mRNAs and proteins are color-coded according to their association with the Notch (blue), FGF (orange) and Wnt (magenta) signaling pathways (based on published literature). Dashed lines indicate regulatory interactions based on literature.

function as transcriptional repressors in the segmentation clock. Cyclic orthologs of the Hes/Her genes also exist in medaka (Elmasri et al., 2004) and *Xenopus* (Li et al., 2003), as well as in the invertebrates *Strigamia* (Chipman and Akam, 2008) and cockroach (Pueyo et al., 2008), suggesting that oscillations of Hes/Her transcription factors in the precursors of the segmented body might represent a shared ancestral trait of bilaterians. The Hes/Her genes might thus represent a segmentation 'kernel' linked to conserved Notch/FGF/Wnt 'plug-ins' in the segmentation gene regulatory network (Davidson and Erwin, 2006).

Despite a remarkable conservation of the periodic activation of the Notch, FGF and Wnt pathways in the three vertebrate species studied, very limited conservation of the individual cyclic genes was observed. Such evolutionary network plasticity might arise from the ability of a robust system, such as the segmentation network (Oates and Ho, 2002), to shield and accumulate mutations, producing so-called cryptic variation (Felix and Wagner, 2008). This scenario is best understood for the vulval induction network in nematodes, where different strains of *C. elegans* show a robust phenotypic output of vulval cell differentiation. Despite similar activation patterns of the Notch, Ras and Wnt pathways, an underlying cryptic variation in the networks of the different strains is revealed via differing sensitivity to perturbations (Milloz et al., 2008). Evolutionary comparison of cell cycle genes identified by microarray time series in *S. pombe*, *S. cerevisiae*, human and *A. thaliana* (Jensen et al., 2006) revealed a limited conservation of individual cycling genes across the four species, in spite of the global conservation of the process and of the molecular players involved. For several protein complexes involved in cell cycle regulation, it appears that only specific subunits are cyclically produced. This principle, called 'just-in-time assembly', provides a simple way to ensure that the complex is rhythmically produced. This enhances evolutionary flexibility because the periodic output of the complex can be achieved via the periodic regulation of any of the members of the complex. The similarity of this scenario

to our findings suggests that just-in-time assembly might be a general mechanism for maintaining oscillations in a system despite changes to the underlying transcriptional program.

In conclusion, our data indicate a striking evolutionary plasticity in the genetic network of the Wnt, FGF and Notch pathways associated with the segmentation clock during vertebrate evolution. Thus, in conserving the segmented architecture of the vertebral column, selection appears restricted to the rhythmic activation of the three pathways, rather than to the expression of individual genes.

Acknowledgements
We thank J. Pace for help; A. Aulehla, M. Labouesse, P. Tomancak, A. Kalinka and members of the A.C.O. and O.P. labs for helpful comments; and the Stowers Institute for Medical Research and the Max Planck Institute of Molecular Cell Biology and Genetics (MPI-CBG) microarray, sequencing, fish and mouse facilities for their excellent support. This research was supported by the Howard Hughes Medical Institute, the Stowers Institute for Medical Research, NIH grant R02 HD043158 (to O.P.) and in part by Defense Advanced Research Projects Agency grant HR 0011-05-1-0057 (to O.P.), a Chaire d'excellence ANR (to O.P.), the Max Planck Society and by the European Research Council under the European Communities Seventh Framework Programme (FP7/2007-2013)/ERC grant 207634 (to A.C.O.). Deposited in PMC for release after 6 months.

Competing interests statement
The authors declare no competing financial interests.

Supplementary material
Supplementary material for this article is available at
http://dev.biologists.org/lookup/suppl/doi:10.1242/dev.063834/-/DC1

References

Ashburner, M., Ball, C. A., Blake, J. A., Botstein, D., Butler, H., Cherry, J. M., Davis, A. P., Dolinski, K., Dwight, S. S., Eppig, J. T. et al. (2000). Gene ontology: tool for the unification of biology. The Gene Ontology Consortium. *Nat. Genet.* **25**, 25-29.
Aulehla, A. and Johnson, R. L. (1999). Dynamic expression of lunatic fringe suggests a link between notch signaling and an autonomous cellular oscillator driving somite segmentation. *Dev. Biol.* **207**, 49-61.
Bell, S. M., Schreiner, C. M., Waclaw, R. R., Campbell, K., Potter, S. S. and Scott, W. J. (2003). Sp8 is crucial for limb outgrowth and neuropore closure. *Proc. Natl. Acad. Sci. USA* **100**, 12195-12200.
Beltman, J., McCormick, F. and Cook, S. J. (1996). The selective protein kinase C inhibitor, Ro-31-8220, inhibits mitogen-activated protein kinase phosphatase-1 (MKP-1) expression, induces c-Jun expression, and activates Jun N-terminal kinase. *J. Biol. Chem.* **271**, 27018-27024.
Benjamini, Y., Drai, D., Elmer, G., Kafkafi, N. and Golani, I. (2001). Controlling the false discovery rate in behavior genetics research. *Behav. Brain Res.* **125**, 279-284.
Berglund, A. C., Sjolund, E., Ostlund, G. and Sonnhammer, E. L. (2008). InParanoid 6, eukaryotic ortholog clusters with inparalogs. *Nucleic Acids Res.* **36**, D263-D266.
Bessho, Y., Hirata, H., Masamizu, Y. and Kageyama, R. (2003). Periodic repression by the bHLH factor Hes7 is an essential mechanism for the somite segmentation clock. *Genes Dev.* **17**, 1451-1456.
Bolstad, B. M., Collin, F., Brettschneider, J., Simpson, K., Cope, L., Irizarry, R. A. and Speed, T. P. (2005). Quality assessment of Affymetrix GeneChip data in bioinformatics and computational biology solutions using R and Bioconductor. In *Bioinformatics and Computational Biology Solutions Using R and Bioconductor* (ed. S. N. York), pp. 33-48. New York: Springer.
Bult, C. J., Eppig, J. T., Kadin, J. A., Richardson, J. E. and Blake, J. A. (2008). The Mouse Genome Database (MGD): mouse biology and model systems. *Nucleic Acids Res.* **36**, D724-D728.
Burks, P. J., Isaacs, H. V. and Pownall, M. E. (2009). FGF signalling modulates transcriptional repression by Xenopus groucho-related-4. *Biol. Cell* **101**, 301-308.
Chipman, A. D. and Akam, M. (2008). The segmentation cascade in the centipede Strigamia maritima: involvement of the Notch pathway and pair-rule gene homologues. *Dev. Biol.* **319**, 160-169.
Chu, Y., Solski, P. A., Khosravi-Far, R., Der, C. J. and Kelly, K. (1996). The mitogen-activated protein kinase phosphatases PAC1, MKP-1, and MKP-2 have unique substrate specificities and reduced activity in vivo toward the ERK2 sevenmaker mutation. *J. Biol. Chem.* **271**, 6497-6501.
Colland, F., Jacq, X., Trouplin, V., Mougin, C., Groizeleau, C., Hamburger, A., Meil, A., Wojcik, J., Legrain, P. and Gauthier, J. M. (2004). Functional proteomics mapping of a human signaling pathway. *Genome Res.* **14**, 1324-1332.
Dale, J. K., Malapert, P., Chal, J., Vilhais-Neto, G., Maroto, M., Johnson, T., Jayasinghe, S., Trainor, P., Herrmann, B. and Pourquie, O. (2006). Oscillations of the snail genes in the presomitic mesoderm coordinate segmental patterning and morphogenesis in vertebrate somitogenesis. *Dev. Cell* **10**, 355-366.
Davidson, E. H. and Erwin, D. H. (2006). Gene regulatory networks and the evolution of animal body plans. *Science* **311**, 796-800.
Dehner, M., Hadjihannas, M., Weiske, J., Huber, O. and Behrens, J. (2008). Wnt signaling inhibits Forkhead box O3a-induced transcription and apoptosis through up-regulation of serum- and glucocorticoid-inducible kinase 1. *J. Biol. Chem.* **283**, 19201-19210.
Dequeant, M. L. and Pourquie, O. (2008). Segmental patterning of the vertebrate embryonic axis. *Nat. Rev. Genet.* **9**, 370-382.
Dequeant, M. L., Glynn, E., Gaudenz, K., Wahl, M., Chen, J., Mushegian, A. and Pourquie, O. (2006). A complex oscillating network of signaling genes underlies the mouse segmentation clock. *Science* **314**, 1595-1598.
Elmasri, H., Liedtke, D., Lucking, G., Volff, J. N., Gessler, M. and Winkler, C. (2004). her7 and hey1, but not lunatic fringe show dynamic expression during somitogenesis in medaka (Oryzias latipes). *Gene Expr. Patterns* **4**, 553-559.
Felix, M. A. and Wagner, A. (2008). Robustness and evolution: concepts, insights and challenges from a developmental model system. *Heredity* **100**, 132-140.
Furthauer, M., Reifers, F., Brand, M., Thisse, B. and Thisse, C. (2001). sprouty4 acts in vivo as a feedback-induced antagonist of FGF signaling in zebrafish. *Development* **128**, 2175-2186.
Furushima, K., Yamamoto, A., Nagano, T., Shibata, M., Miyachi, H., Abe, T., Ohshima, N., Kiyonari, H. and Aizawa, S. (2007). Mouse homologues of Shisa antagonistic to Wnt and Fgf signalings. *Dev. Biol.* **306**, 480-492.
Gibb, S., Zagorska, A., Melton, K., Tenin, G., Vacca, I., Trainor, P., Maroto, M. and Dale, J. K. (2009). Interfering with Wnt signalling alters the periodicity of the segmentation clock. *Dev. Biol.* **330**, 21-31.
Glynn, E. F., Chen, J. and Mushegian, A. R. (2006). Detecting periodic patterns in unevenly spaced gene expression time series using Lomb-Scargle periodograms. *Bioinformatics* **22**, 310-316.
Goldbeter, A. and Pourquie, O. (2008). Modeling the segmentation clock as a network of coupled oscillations in the Notch, Wnt and FGF signaling pathways. *J. Theor. Biol.* **252**, 574-585.
Griffin, K. J., Amacher, S. L., Kimmel, C. B. and Kimelman, D. (1998). Molecular identification of spadetail: regulation of zebrafish trunk and tail mesoderm formation by T-box genes. *Development* **125**, 3379-3388.
Guemar, L., de Santa Barbara, P., Vignal, E., Maurel, B., Fort, P. and Faure, S. (2007). The small GTPase RhoV is an essential regulator of neural crest induction in Xenopus. *Dev. Biol.* **310**, 113-128.
Hamburger, V. and Hamilton, H. L. (1992). A series of normal stages in the development of the chick embryo. 1951. *Dev. Dyn.* **195**, 231-272.
Henrique, D., Adam, J., Myat, A., Chitnis, A., Lewis, J. and Ish-Horowicz, D. (1995). Expression of a Delta homologue in prospective neurons in the chick. *Nature* **375**, 787-790.
Henry, C. A., Urban, M. K., Dill, K. K., Merlie, J. P., Page, M. F., Kimmel, C. B. and Amacher, S. L. (2002). Two linked hairy/Enhancer of split-related zebrafish genes, her1 and her7, function together to refine alternating somite boundaries. *Development* **129**, 3693-3704.
Holley, S. A., Geisler, R. and Nusslein-Volhard, C. (2000). Control of her1 expression during zebrafish somitogenesis by a delta-dependent oscillator and an independent wave-front activity. *Genes Dev.* **14**, 1678-1690.
Hong, S. K. and Dawid, I. B. (2009). FGF-dependent left-right asymmetry patterning in zebrafish is mediated by Ier2 and Fibp1. *Proc. Natl. Acad. Sci. USA* **106**, 2230-2235.
Hubbard, T. J., Aken, B. L., Ayling, S., Ballester, B., Beal, K., Bragin, E., Brent, S., Chen, Y., Clapham, P., Clarke, L. et al. (2009). Ensembl 2009. *Nucleic Acids Res.* **37**, D690-D697.
Issack, P. S. and Ziff, E. B. (1998). Altered expression of helix-loop-helix transcriptional regulators and cyclin D1 in Wnt-1-transformed PC12 cells. *Cell Growth Differ.* **9**, 837-845.
Jensen, L. J., Jensen, T. S., de Lichtenberg, U., Brunak, S. and Bork, P. (2006). Co-evolution of transcriptional and post-translational cell-cycle regulation. *Nature* **443**, 594-597.
Jiang, Y. J., Aerne, B. L., Smithers, L., Haddon, C., Ish-Horowicz, D. and Lewis, J. (2000). Notch signalling and the synchronization of the somite segmentation clock. *Nature* **408**, 475-479.
Jouve, C., Palmeirim, I., Henrique, D., Beckers, J., Gossler, A., Ish-Horowicz, D. and Pourquie, O. (2000). Notch signalling is required for cyclic expression of the hairy-like gene HES1 in the presomitic mesoderm. *Development* **127**, 1421-1429.
Kanehisa, M., Goto, S., Furumichi, M., Tanabe, M. and Hirakawa, M. (2010). KEGG for representation and analysis of molecular networks involving diseases and drugs. *Nucleic Acids Res.* **38**, D355-D360.
Kumar, S. R., Scehnet, J. S., Ley, E. J., Singh, J., Krasnoperov, V., Liu, R., Manchanda, P. K., Ladner, R. D., Hawes, D., Weaver, F. A. et al. (2009).

Preferential induction of EphB4 over EphB2 and its implication in colorectal cancer progression. *Cancer Res.* **69**, 3736-3745.
Latinkic, B. V., Mercurio, S., Bennett, B., Hirst, E. M., Xu, Q., Lau, L. F., Mohun, T. J. and Smith, J. C. (2003). Xenopus Cyr61 regulates gastrulation movements and modulates Wnt signalling. *Development* **130**, 2429-2441.
Leimeister, C., Dale, K., Fischer, A., Klamt, B., Hrabe de Angelis, M., Radtke, F., McGrew, M. J., Pourquie, O. and Gessler, M. (2000). Oscillating expression of c-hey2 in the presomitic mesoderm suggests that the segmentation clock may use combinatorial signaling through multiple interacting bHLH factors. *Dev. Biol.* **227**, 91-103.
Lewis, J. (2003). Autoinhibition with transcriptional delay: a simple mechanism for the zebrafish somitogenesis oscillator. *Curr. Biol.* **13**, 1398-1408.
Li, Y., Fenger, U., Niehrs, C. and Pollet, N. (2003). Cyclic expression of esr9 gene in Xenopus presomitic mesoderm. *Differentiation* **71**, 83-89.
Liu, Y. P., Burleigh, D., Durning, M., Hudson, L., Chiu, I. M. and Golos, T. G. (2004). Id2 is a primary partner for the E2-2 basic helix-loop-helix transcription factor in the human placenta. *Mol. Cell. Endocrinol.* **222**, 83-91.
Maglott, D., Ostell, J., Pruitt, K. D. and Tatusova, T. (2007). Entrez Gene: gene-centered information at NCBI. *Nucleic Acids Res.* **35**, D26-D31.
McCurley, A. T. and Callard, G. V. (2008). Characterization of housekeeping genes in zebrafish: male-female differences and effects of tissue type, developmental stage and chemical treatment. *BMC Mol. Biol.* **9**, 102.
McGrew, M. J., Dale, J. K., Fraboulet, S. and Pourquie, O. (1998). The lunatic fringe gene is a target of the molecular clock linked to somite segmentation in avian embryos. *Curr. Biol.* **8**, 979-982.
Milloz, J., Duveau, F., Nuez, I. and Felix, M. A. (2008). Intraspecific evolution of the intercellular signaling network underlying a robust developmental system. *Genes Dev.* **22**, 3064-3075.
Moreno-Risueno, M. A., Van Norman, J. M., Moreno, A., Zhang, J., Ahnert, S. E. and Benfey, P. N. (2010). Oscillating gene expression determines competence for periodic Arabidopsis root branching. *Science* **329**, 1306-1311.
Oates, A. C. and Ho, R. K. (2002). Hairy/E(spl)-related (Her) genes are central components of the segmentation oscillator and display redundancy with the Delta/Notch signaling pathway in the formation of anterior segmental boundaries in the zebrafish. *Development* **129**, 2929-2946.
Ozbudak, E. M., Tassy, O. and Pourquie, O. (2010). Spatiotemporal compartmentalization of key physiological processes during muscle precursor differentiation. *Proc. Natl. Acad. Sci. USA* **107**, 4224-4229.
Palmeirim, I., Henrique, D., Ish-Horowicz, D. and Pourquié, O. (1997). Avian hairy gene expression identifies a molecular clock linked to vertebrate segmentation and somitogenesis. *Cell* **91**, 639-648.
Picker, A., Roellig, D., Pourquie, O., Oates, A. C. and Brand, M. (2009). Tissue micromanipulation in zebrafish embryos. *Methods Mol. Biol.* **546**, 153-172.
Pueyo, J. I., Lanfear, R. and Couso, J. P. (2008). Ancestral Notch-mediated segmentation revealed in the cockroach Periplaneta americana. *Proc. Natl. Acad. Sci. USA* **105**, 16614-16619.
Shankaran, S. S., Sieger, D., Schroter, C., Czepe, C., Pauly, M. C., Laplante, M. A., Becker, T. S., Oates, A. C. and Gajewski, M. (2007). Completing the set of h/E(spl) cyclic genes in zebrafish: her12 and her15 reveal novel modes of expression and contribute to the segmentation clock. *Dev. Biol.* **304**, 615-632.
Sieger, D., Tautz, D. and Gajewski, M. (2004). her11 is involved in the somitogenesis clock in zebrafish. *Dev. Genes Evol.* **214**, 393-406.
Sprague, J., Bayraktaroglu, L., Clements, D., Conlin, T., Fashena, D., Frazer, K., Haendel, M., Howe, D. G., Mani, P., Ramachandran, S. et al. (2006). The Zebrafish Information Network: the zebrafish model organism database. *Nucleic Acids Res.* **34**, D581-D585.
Tang, L. Y., Deng, N., Wang, L. S., Dai, J., Wang, Z. L., Jiang, X. S., Li, S. J., Li, L., Sheng, Q. H., Wu, D. Q. et al. (2007a). Quantitative phosphoproteome profiling of Wnt3a-mediated signaling network: indicating the involvement of ribonucleoside-diphosphate reductase M2 subunit phosphorylation at residue serine 20 in canonical Wnt signal transduction. *Mol. Cell. Proteomics* **6**, 1952-1967.
Tang, R., Dodd, A., Lai, D., McNabb, W. C. and Love, D. R. (2007b). Validation of zebrafish (Danio rerio) reference genes for quantitative real-time RT-PCR normalization. *Acta Biochem. Biophys. Sinica* **39**, 384-390.
Thisse, C., Thisse, B., Schilling, T. F. and Postlethwait, J. H. (1993). Structure of the zebrafish snail1 gene and its expression in wild-type, spadetail and no tail mutant embryos. *Development* **119**, 1203-1215.
Thorpe, C. J., Weidinger, G. and Moon, R. T. (2005). Wnt/beta-catenin regulation of the Sp1-related transcription factor sp5l promotes tail development in zebrafish. *Development* **132**, 1763-1772.
Traina, F., Favaro, P. M., Medina Sde, S., Duarte Ada, S., Winnischofer, S. M., Costa, F. F. and Saad, S. T. (2006). ANKHD1, ankyrin repeat and KH domain containing 1, is overexpressed in acute leukemias and is associated with SHP2 in K562 cells. *Biochim. Biophys. Acta* **1762**, 828-834.
Wilson, D., Charoensawan, V., Kummerfeld, S. K. and Teichmann, S. A. (2008). DBD-taxonomically broad transcription factor predictions: new content and functionality. *Nucleic Acids Res.* **36**, D88-D92.
Wright, D., Ferjentsik, Z., Chong, S. W., Qiu, X., Jiang, Y. J., Malapert, P., Pourquie, O., Van Hateren, N., Wilson, S. A., Franco, C. et al. (2009). Cyclic Nrarp mRNA expression is regulated by the somitic oscillator but Nrarp protein levels do not oscillate. *Dev. Dyn.* **238**, 3043-3055.
Zeeberg, B. R., Feng, W., Wang, G., Wang, M. D., Fojo, A. T., Sunshine, M., Narasimhan, S., Kane, D. W., Reinhold, W. C., Lababidi, S. et al. (2003). GoMiner: a resource for biological interpretation of genomic and proteomic data. *Genome Biol.* **4**, R28.
Zhao, H., Tanegashima, K., Ro, H. and Dawid, I. B. (2008a). Lrig3 regulates neural crest formation in Xenopus by modulating Fgf and Wnt signaling pathways. *Development* **135**, 1283-1293.
Zhao, X., Heng, J. I., Guardavaccaro, D., Jiang, R., Pagano, M., Guillemot, F., Iavarone, A. and Lasorella, A. (2008b). The HECT-domain ubiquitin ligase Huwe1 controls neural differentiation and proliferation by destabilizing the N-Myc oncoprotein. *Nat. Cell Biol.* **10**, 643-653.